Cement and Concrete Research 42 (2012) 333–343

Contents lists available at SciVerse ScienceDirect

Cement and Concrete Research

journal homepage: http://ees.elsevier.com/CEMCON/default.asp

Chemical and mechanical stability of sodium sulfate activated slag after exposure to elevated temperature

A.M. Rashad [a,*], Y. Bai [b,*], P.A.M. Basheer [b], N.C. Collier [c], N.B. Milestone [c]

[a] Housing & Building National Research Center, HBRC, 87 El-Tahrir St., Dokki, Giza 11511, P.O. Box: 1770, Cairo, Egypt
[b] School of Planning, Architecture & Civil Engineering, Queen's University Belfast, David Keir Building, Stranmillis Road, Belfast BT9 5AG, UK
[c] Immobilisation Science Laboratory, Department of Engineering Materials, The University of Sheffield, Mappin Street, Sheffield S1 3JD, UK

ARTICLE INFO

Article history:
Received 11 May 2011
Accepted 16 October 2011

Keywords:
Activated slag (D)
Elevated temperature (A)
pH value (A)
Residual compressive strength (C)
Sodium sulfate (D)

ABSTRACT

The chemical and mechanical stability of slag activated with two different concentrations of sodium sulfate (Na_2SO_4) after exposure to elevated temperatures ranging from 200 to 800 °C with an increment of 200 °C has been examined. Compressive strengths and pH of the hardened pastes before and after the exposure were determined. The various decomposition phases formed were identified using X-ray diffraction, thermogravimetric analysis and scanning electron microscopy. The results indicated that Na_2SO_4 activated slag has a better resistance to the degradation caused by exposure to elevated temperature up to 600 °C than Portland cement system as its relative strengths are superior. The finer slag and higher Na_2SO_4 concentration gave better temperature resistance. Whilst the pH of the hardened pastes decreased with an increase in temperature, it still maintained a sufficiently high pH for the protection of reinforcing bar against corrosion.

1. Introduction

The resistance of concrete made with Portland cement (PC) to degradation caused by exposure to elevated temperatures depends on the type of material used in the concrete. The least stable constituent in this respect is the hardened cement paste. Both chemical and physical deteriorations occur at elevated temperatures because both interlayer and chemically bound water are lost due to the decomposition of calcium hydroxide (CH) and calcium silicate hydrate (C-S-H) [1]. The porosity and mineralogy of the aggregate also affect the severity of deteriorations [2].

It has been shown that the critical exposure temperature at which concrete begins to lose compressive strength is approximately 400 °C. This is caused by the decomposition of CH and the consequent volume increase that occurs during cooling when rehydration of calcium oxide initiates a volume increase by about 44%, leading to cracking [3]. Handoo et al. [4] reported that the loss of strength in PC concretes after 400 °C could be attributed to the loss of crystalline water, resulting in the decomposition of the calcium hydroxide. Georgali and Tsakiridis [5] attributed the cracking and softening of the concrete surface exposed to fire to the expansion followed by the shrinkage of PC paste due to the transformation of calcium hydroxide to calcium oxide in the temperature range of 450–500 °C. Petzold and Rohrs [6] explained that the loss of strength can be attributed to the rehydration of calcium oxide, which is accompanied by a 44% increase in volume. In addition, the explosive spalling that can occur [7,8] at temperatures between 480 and 510 °C [9], will reduce the loading capacity of concrete structures. The different effects of exposure of cement paste to elevated temperatures have been summarized as follows [10]:

- capillary and gel water evaporate at ~100–150 °C,
- shrinkage and cracking take place at approximately ~150–250 °C accompanied by a reduction in tensile strength,
- evaporation of chemically bound water from aluminous and ferrous constituents at approximately ~250–300 °C, and the compressive strength of concrete starts to decrease.
- CH dehydrates to calcium oxide at approximately ~400 °C with an accompanying 44% reduction of the volume and a reduction in strength,
- C-S-H finishes decomposition between approximately ~400–600 °C, and strength reduction becomes significant.

PC is produced by a highly energy intensive process and a major contributor of greenhouse gases responsible for about 5–8% of all global carbon dioxide emissions. Ground granulated blast furnace slag (GGBS) is a by-product of iron manufacturing using blast-furnaces [11] and is normally used to replace PC. The manufacture of GGBS is more environmentally friendly than that of PC, which requires less than one fifth of the energy to produce, generates one fifteenth of carbon dioxide emissions and does not require quarrying of virgin materials. Currently, the UK uses about 2 million tonnes per annum of GGBS in cement, which:

- reduces carbon dioxide emissions by about 2 million tonnes.

* Corresponding authors.
E-mail addresses: alaarashad@yahoo.com (A.M. Rashad), y.bai@qub.ac.uk (Y. Bai).

0008-8846/$ – see front matter © 2011 Elsevier Ltd. All rights reserved.
doi:10.1016/j.cemconres.2011.10.007

– reduces primary energy use by 2000 million kWh
– saves 3 million tonnes of quarrying
– saves a potential landfill of nearly 2 million tonnes.

The use of slag as a partial replacement of Portland cement (PC) in blended cements and in ready mixed concrete not only consumes large amount of unused waste produced by the steel industry, but also reduces the carbon dioxide emissions arising from cement manufacture and reduces the energy required by the cement industry. Portland cement blended with slag is usually used to modify the properties of cement and concrete. Wang [12] reported that, the substitution of PC with GGBS improves compressive strength and reduces cracking at elevated temperatures. The optimum cement replacement in this study was 80% at a water/binder ratio of 0.23. Another study on blended cement [13] concluded that, when cement was blended with slag, the reduction in CH produced during hydration led to improved mechanical properties following exposure to temperatures in excess of 400 °C. A similar study by Khoury et al. [14] showed that the addition of 50% slag to a sulfate — resisting Portland cement reduced the amount of CH formed during the hydration, which consequently increased the fire resistance of the paste samples containing 50% slag when exposed to approximately 550 °C. Other researchers have also shown the useful contribution of slag to high temperature resistance [15–19].

Slag can also be used to formulate non Portland cement binders consisting of only slag plus an activator, a system called alkali-activated slags (AAS) [20]. Usually strong alkalis, such as NaOH and/or sodium silicate are used as the activators. Weak alkaline salts such as Na_2CO_3 or neutral salts such as Na_2SO_4 also function in a similar way. Compared to PC the CH is usually not formed in the hydrated AAS [20–23], so it is expected that alkali-activated slag concrete has a higher resistance to elevated temperatures compared to PC concrete or blended cement concrete made with slag. However, there are very few publications in the literature which have studied the effect of elevated temperature on alkali-activated slag. The first study used sodium hydroxide as an activator and exposure temperatures up to 800 °C [21]. The compressive strength results from this study have indicated that the alkali-activated slag concrete remained about 25% of its original strength after exposure to 800 °C which was similar to Portland cement concrete. De Gutierrez et al. [24] concluded that regardless of the type of activator, the residual strength of alkali-activated slag up to 1000 °C was similar to that of the PC mix. They considered that the dehydration of calcium silicate hydrate was the reason for the strength loss in a manner similar to the PC. Other studies [22,24–26] investigated the fire performance of sodium silicate powder activated slag mortars up to 1200 °C using quartz [22,25,26] and electrical porcelain [25,26] as aggregates. They reported that the remaining strengths were approximately 20% at 800 °C. However, between 800 and 1200 °C the strength of the alkali-activated slag mortar with quartz aggregate increased. At 1200 °C, it reached about 87% of its original strength. The alkali-activated slag mortar with electrical porcelain experienced a doubling of its original strength between 800 and 1200 °C. Zuda et al. [27] studied the thermal properties of alkali-activated slag mortars activated by sodium silicate subjected to elevated temperatures up to 1200 °C. This study has concluded that, the alkali-activated slag mortar had a good potential for future high temperature applications in civil engineering where thermal diffusivity and thermal conductivity decreased above 400 °C with the increase of temperature. Recently, Guerrieri et al. [28] studied the residual compressive strength of slag concrete activated by sodium silicate powder and hydrated lime after exposure to temperatures up to 1200 °C. The results illustrated that the residual compressive strength of the concrete was approximately 76, 73, 46 and 10% of the originals when exposed to 200, 400, 600 and 800 °C respectively.

Bernal et al. [29] studied the effect of elevated temperatures of 200, 400, 600, 800 and 1000 °C for 2 h on geopolymers formulated with an overall SiO_2/Al_2O_3 molar ratio of 3, slag/(slag + metakaolin) ratios of 0.0 and 0.2, constant H_2O/Na_2O ratio of 12 and Na_2O/SiO_2 ratio of 0.25. The results have indicated that the geopolymers formulated with metakaolin (MK) and slag have higher residual compressive strength than the pure MK-based geopolymer up to 800 °C. On the other hand, the pure MK system showed a much higher residual strength upon cooling from 1000 °C to room temperature, indicating that the extent of glass formation from the geopolymer gel at 1000 °C is reduced by the incorporation of Ca into the gel, as a consequence of formation of C-S-H type gel that coexists with the aluminosilicate geopolymer gel. Other several studies have been reported regarding the performance of alkali-activated slags under high temperature [23,30–32]. These studies have found that alkali-activated systems, independent of the precursor used but particularly in the geopolymer systems, generally show a higher stability than Portland cement when exposed to high temperatures. This is attributed to the presence of a highly condensed binder gel, the low content of chemically bonded water in the alkali-activated gel products and the absence of CH as a reaction product in the majority of the systems. This means that alkali-activated binder can provide an attractive technological alternative to Portland cement in applications where stability at high temperatures is required.

The review of the literature has clearly indicated that there are few publications comparing the performance of alkali-activated slag with PC-based systems under elevated temperatures. In particular, until now, there has not been any publication studying the behaviour of sodium sulfate activated slag exposed to elevated temperatures. In recent years, sodium sulfate activated slag has attracted considerable attention from both the construction and waste management industry due to some of its unique properties compared to the slag activated by other activators, such as reduced heat of hydration and reduced cost. For both applications, a good understanding of its performance under elevated temperatures is essential. Therefore, the main goal of this research was to study the effect of elevated temperatures on the chemical stability and residual compressive strength of slag pastes manufactured with sodium sulfate activated slag, which was also compared with a paste manufactured with PC.

2. Experimental details

An experimental programme was designed to investigate the chemical stability and the residual strength of sodium sulfate activated slag, after being exposed to elevated temperatures. A ground granulated blast furnace slag (GGBS) with different fineness was activated by sodium sulfate at two different concentrations, namely 1% and 3% (Na_2O equivalent), by the mass of the GGBS. One Portland cement mix was employed as a reference. In total, five paste mixes were prepared. Each mix comprised seven groups, with each consisting of three samples. The first and second groups were tested directly in room temperature condition after curing at the ages of 3 and 7 days to determine the early age compressive strengths. The third group was tested directly in the room temperature condition after curing at the age of 28 days to determine the reference or control compressive strength. The fourth, fifth, sixth and seventh groups were tested after being exposed to elevated temperatures ranging from 200 to 800 °C, at temperature increments of 200 °C at a rate of 4 °C/min and keeping for a constant period of exposure time of 2 h at each temperature.

2.1. Materials

From here on, the term “slag” will be used to refer to ground granulated blast-furnace slag (GGBS). A slag with two different

finenesses, 2500 and 5000 cm^2/g, supplied by UK Hanson Cement was used in this research to manufacture the sodium sulfate activated slag pastes. Analytical grade sodium sulfate was used as an activator. The Portland cement, CEMI class 42.5R with a Blaine surface area of 2700 cm^2/g and complying with Irish Standard I.S. EN 197-1: 2001, supplied by Irish Cement Ltd, was employed as a reference. The chemical composition of cementitious materials characterised by X-ray fluorescence (XRF) analysis are given in Table 1. The specific gravity and the bulk density of the slag were 2.8 and 1200 kg/m^3, respectively.

2.2. Mix proportions

Four sodium sulfate activated slag pastes and a reference PC paste were prepared. The details of each mix are presented in Table 2. The water-to-binder ratio, W/B, was fixed at 0.3 for all the mixes.

2.3. Casting, curing, heat regimes and testing

The slag was dried in a special dryer for 6 h at 40 (±1) °C before mixing. The sodium sulfate solution was prepared and used at 40 (±1) °C. The slag was added to the sodium sulfate solution, previously placed in the bowl of a Hobart planetary mixer, over a 5 min period after which time the mixer was stopped and any unmixed powders were scraped off the sides and paddled into the mixing bowl. Mixing was then continued for another 5 min before casting in 50 mm cube moulds and vibrated for 1 min to remove air bubbles. The same mixing regime was applied to the PC pastes. Each specimen along with the steel mould was wrapped with a damp hessian cloth before being sealed in a plastic sample bag. All the specimens were then cured at 40 (±1) °C in an environmental chamber for 3 days before removing the cubes from the steel moulds. Each cube was then again wrapped with a damp hessian cloth, sealed in a plastic sample bag and cured at 40 (±1) °C until they were tested. The damp hessian cloth was regularly checked and replaced if it became dry.

After 3 and 7 days, three required samples were tested in compression and the average value was used to assess their early age compressive strengths. Similarly, after 28 days, three required samples were tested, without being exposed to elevated temperatures, called reference samples, whilst those to be exposed to elevated temperatures were transferred to an oven for drying at 105 (±1) °C for 24 h. The specimens were then placed in a furnace and heated to 200, 400, 600 and 800 °C at a rate of 4 °C/min and held for 2 h at each temperature (see Refs. [22,29,33–43] for further rationale of exposure regimes) in order to investigate the chemical stability and residual compressive strength of the PC and activated slag pastes at each temperature. After exposing to each targeted temperature for 2 h, the specimens were left in the furnace to gradually cool down to room temperature so as to avoid any temperature shock.

The workability of pastes was measured immediately after mixing using a mini-slump test, which uses a small cone with bottom diameter of 38 mm, top diameter of 19 mm and height of 57 mm [44].

The compressive strength was measured at 3, 7 and 28 days by testing triplicate specimens at each age using a loading rate which complies with BS EN 1961: 2005 over the entire load application until failure. The residual compressive strength after heating to elevated temperature and cooling was determined by an unstressed compression test [45].

After the compressive strength test, selected debris from the crushed samples was stored in acetone for three days in order to stop the hydration. The debris was then filtered from the acetone and dried in the desiccators under vacuum. Part of the dried samples was ground in an agate mortar. Particles passing a 63 μm sieve were used for X-ray diffraction (XRD) and thermogravimetric analysis (TGA). Some selected pieces were also analysed using the scanning electron microscopy (SEM).

Table 1
Oxide composition of PC and slag (wt.%) after calculation from XRF results.

Composition	PC	GGBS
CaO	63.47	40.89
SiO_2	20.18	34.94
Al_2O_3	4.83	11.69
MgO	2.47	7.42
Fe_2O_3	3.16	3.32
SO_3	3.26	1.19
K_2O	0.52	0.34
Na_2O	0.16	0.16
TiO_2	0.3	0.49
MnO	0.22	0.27
P_2O_5	0.09	0.01
Loss of ignition	2.18	−0.93

Table 2
Details of paste mix proportions for 100 g of starting materials (PC or slag).

Mix ID	PC (g)	Slag (g)	Slag fineness (cm^2/g)	Na_2SO_4 (g)	Na_2SO_4 concentration (Na_2O equivalent by mass of slag)	Water (g)
M1	100	–	–	–	–	30
M2	–	100	2500	2.29	1%	30
M3	–	100	5000	2.29	1%	30
M4	–	100	2500	6.87	3%	30
M5	–	100	5000	6.87	3%	30

3. Results and discussion

3.1. Initial slump

As it can be seen from Fig. 1, the initial slump of the sodium sulfate activated slag pastes depended on the slag fineness, the slump decreased with an increasing fineness which can be attributed to the increase in surface area with the increase in fineness. However, despite the slag being nearly twice as fine as the PC, the same workability was recorded. It also can be seen that the concentration of the sodium sulfate had no effect on the mini-slump. To determine the reason for these observations, further investigation is needed on the rheological characteristics of the pastes.

3.2. Compressive strength

Fig. 2 illustrates the compressive strength results for the PC and the activated slag pastes. The compressive strength of all the pastes

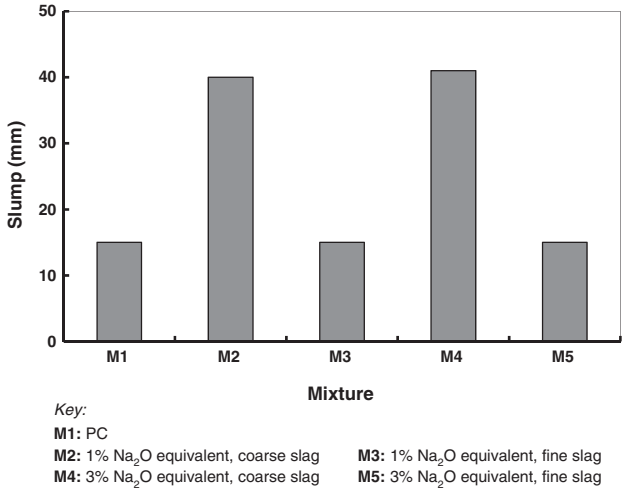

Fig. 1. Initial slump for various mixes.

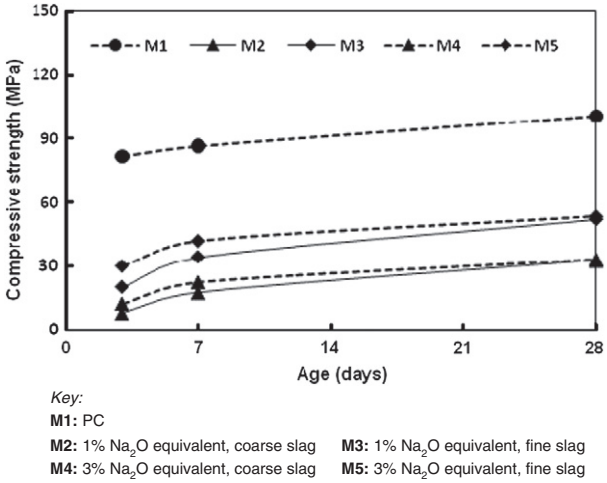

Fig. 2. Compressive strength development of PC and activated slag pastes.

increased with age, but the PC paste gave higher compressive strength than any of the activated pastes. The compressive strength of the activated slag pastes appeared to be highly dependent on the slag fineness and the activator concentration. Increasing slag fineness resulted in a strength gain at all ages regardless of the activator concentration. Increasing the sodium sulfate concentration caused a significant increase in compressive strength at early ages and the highest increase in compressive strength was found at 3 days. By 28 days, the compressive strength of the hardened slag pastes activated by either 1% or 3% Na_2O equivalent of Na_2SO_4 tended to converge to the same value.

3.3. The response of paste mixes to thermal loading

Exposing cementitious products to elevated temperatures is normally associated with multiple chemico-physical transformations, which would affect the stability of the internal structure and consequently the compressive strength. These include dehydration (decomposition) of the cementitious compounds, different thermal expansion values of the constituents (thermal mismatch) and the internal pore pressure [1].

The behaviour of the hardened pastes after exposure to different thermal loads was evaluated quantitatively by measuring the retained (residual) strengths after the heat exposure.

3.3.1. Hardened PC paste

Fig. 3 shows the heat strength profile of PC pastes after being subjected to 200, 400, 600 and 800 °C. It can be seen that the compressive strength of the hardened PC paste increased after being heated at 200 °C for 2 h. However, above 200 °C a decrease in strength was observed. The increase in strength up to 200 °C can be partly attributed to the evaporation of water, leading to an increase in friction between

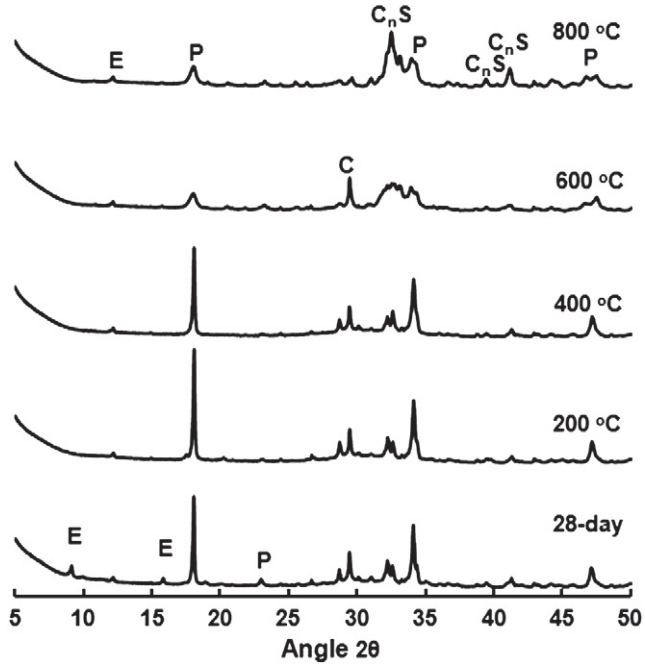

Fig. 4. XRD traces of hardened PC paste after 28-day hydration and after being exposed at different temperatures.

the failure planes, or a gain in strength due to the phenomenon called "dry hardening" [45], which causes a strength increase between 150 and 350 °C. The strengthening of the hydrated cement paste formed during the evaporation of free water, leads to greater Van der Waal's forces as a result of the cement gel layers moving closer to each other [46–48]. The heating process also causes further hydration as a result of steam formation with "internal autoclaving" occurring in the cement paste [49], i.e. increased chemical bounding. Whatever the effect, the relative residual compressive strength was 122.5% of that not exposed to the temperature of 200 °C.

When the temperature was increased from 200 °C to 400 °C, the compressive strength of the hardened PC paste was not affected when compared to its original 28-day compressive strength at room temperature and the relative residual compressive strength was 99.22% of its original at room temperature which was lower than that at 200 °C. When the temperature was increased from 400 °C to 600 °C, further strength loss could be observed, which could be caused by the coarsening of the pore-structure of the hardened cement paste [50–53] and the decompositions of calcium hydroxide (which occurred at approximately 430–600 °C) [53]. Exposing the hardened PC paste to 800 °C caused further reduction of compressive strength which might be due to the ongoing physic-chemical

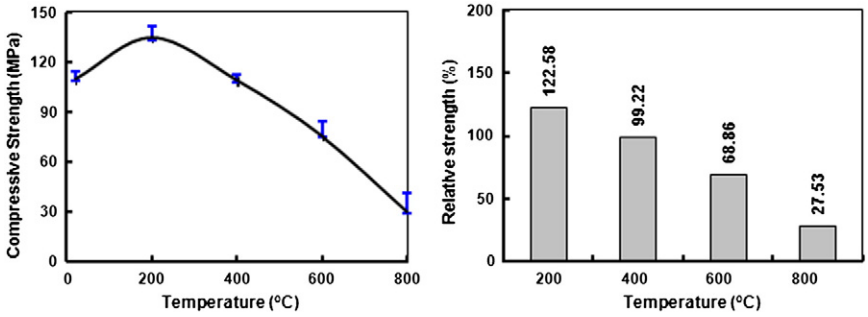

Fig. 3. Heat strength profile of PC pastes.

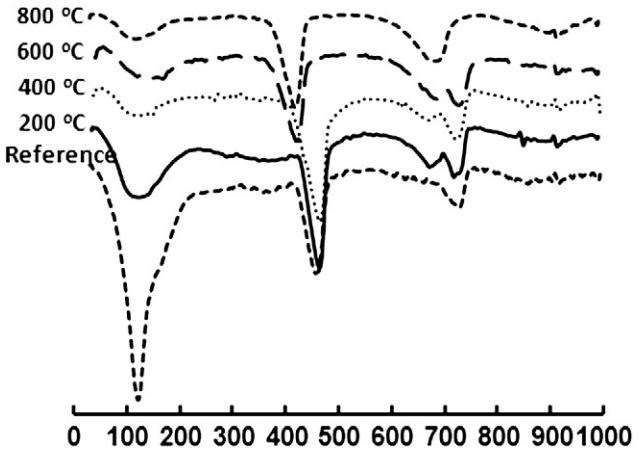

Fig. 5. DTG thermograms of hardened PC pastes after being exposed at different temperatures.

transformations such as crystallization of new compounds and more shrinkage. The loss of strength between approximately 600 and 800 °C could also be attributed to a dramatically increased decomposition of C-S-H which started at 560 °C and became significant above 600 °C [53]. However, the relative residual compressive strengths were 68.9% and 27.5% of the 28-day strength after espousing to 600 and 800 °C respectively.

Fig. 4 illustrates the XRD patterns of the 28-day PC paste at room temperature as well as those after being exposed to 200, 400, 600 and 800 °C respectively. Evidently, the crystalline phase of CH (portlandite) was decreased as the temperature increases up to 800 °C,

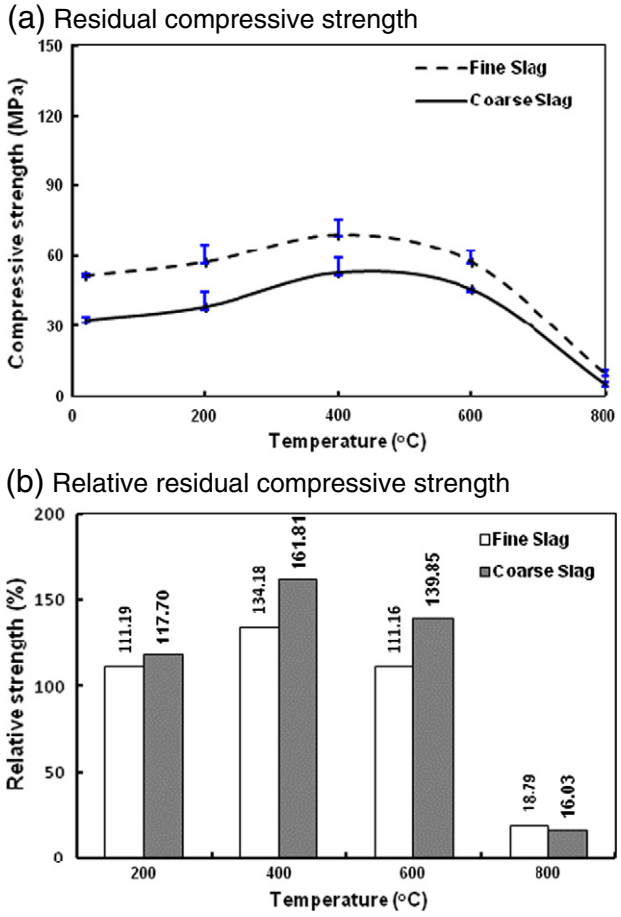

Fig. 6. Heat strength profile of slag pastes activated with 1% Na_2O equivalent of Na_2SO_4.

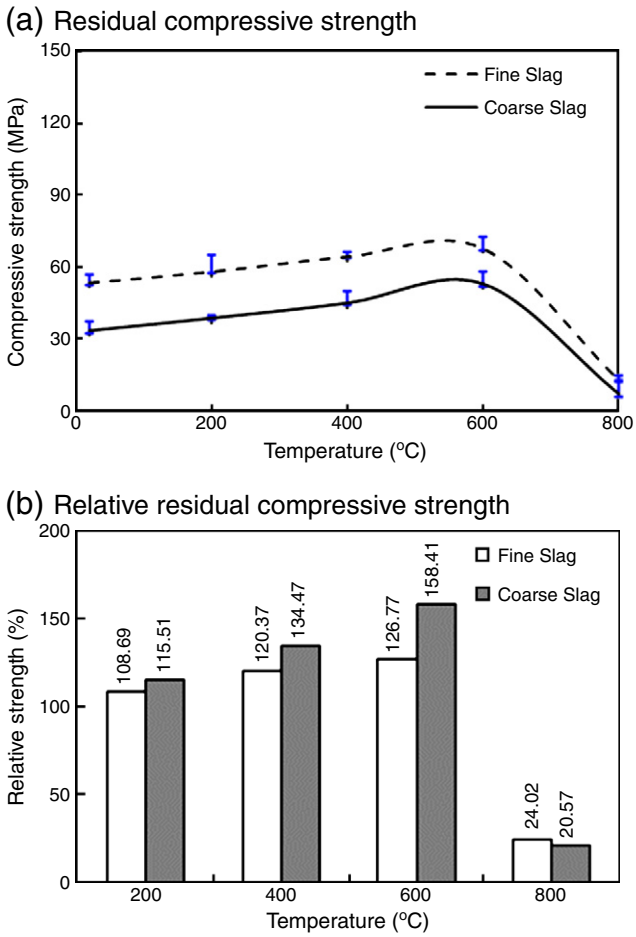

Fig. 7. Heat strength profile of slag pastes activated with 3% Na_2O equivalent of Na_2SO_4.

in particular, a significant reduction in the intensity of CH peak could be observed after the PC being exposed to 600 °C. This is due to the thermal decomposition of calcium hydroxide phase at about 500 °C (as shown in the DTG curve in Fig. 5), forming evaporable water steam ($H_2O\uparrow$) and calcium oxide (CaO) [54]:

$$Ca(OH)_2 \rightarrow CaO + H_2O\uparrow$$

The products formed are porous and could absorb atmospheric water vapour to re-hydrate and re-form $Ca(OH)_2$ accompanied by volume expansion and further cracking, if being exposed to the atmospheric environment [3]. After being exposed to 800 °C, peaks of ß-

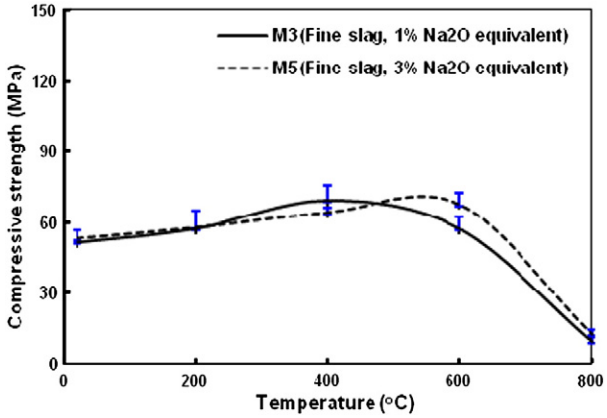

Fig. 8. Effect of Na_2SO_4 concentration on the residual compressive strength of pastes manufactured with fine slag.

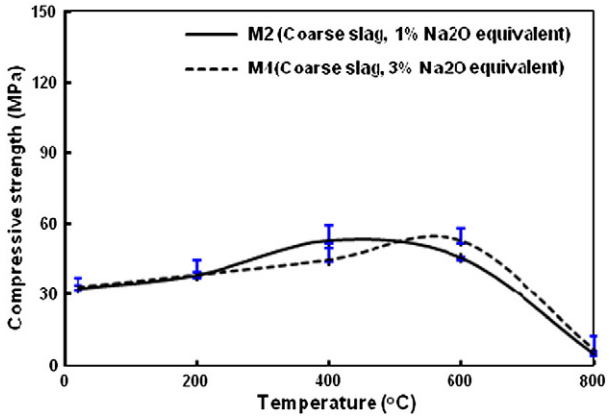

Fig. 9. Effect of Na_2SO_4 concentration on the residual compressive strength of pastes manufactured with coarse slag.

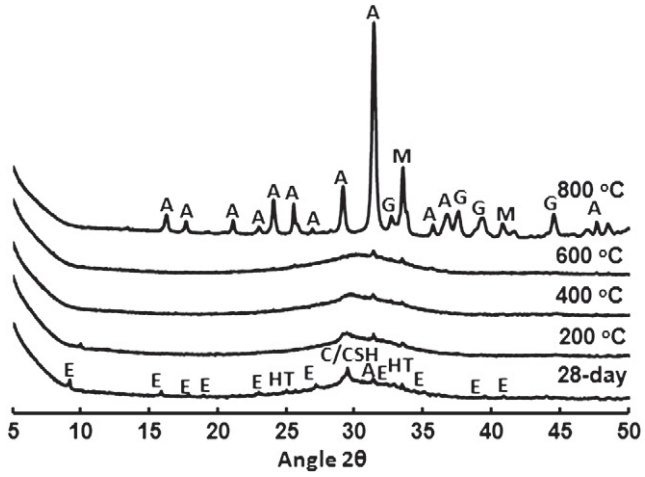

Key: E – ettringite $Ca_6Al_2(SO_4)_3(OH)_{12}\cdot 26H_2O$, HT – hydrotalcite $Mg_6Al_2CO_3(OH)_{16}\cdot 4H_2O$, C/C-S-H – overlapping calcite and calcium silicate hydrate, A – akermanite $Ca_2Mg(Si_2O_7)$, M –merwinite $Ca_3Mg(SiO_4)_2$, G-gehlenite $Ca_2Al(AlSiO_7)$

Fig. 10. X-ray patterns of M2 pastes after 28-day hydration and after being exposed at different temperatures.

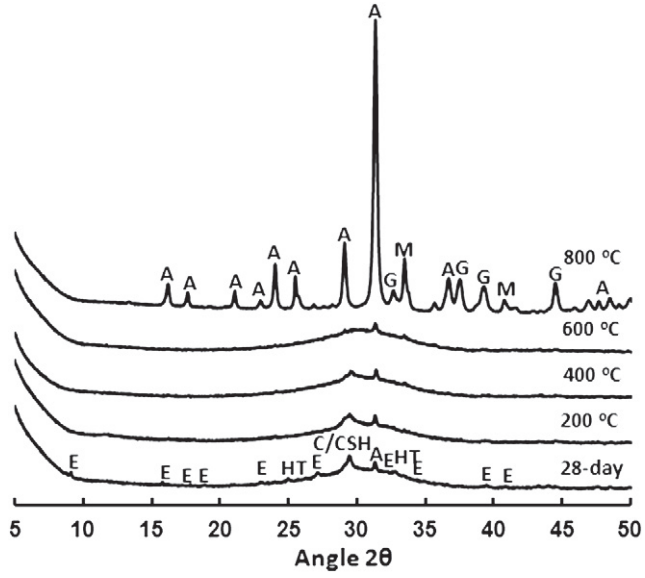

Key: E – ettringite $Ca_6Al_2(SO_4)_3(OH)_{12}\cdot 26H_2O$, HT – hydrotalcite $Mg_6Al_2CO_3(OH)_{16}\cdot 4H_2O$, C/C-S-H – overlapping calcite and calcium silicate hydrate, A – akermanite $Ca_2Mg(Si_2O_7)$, M – merwinite $Ca_3Mg(SiO_4)_2$, G-gehlenite $Ca_2Al(AlSiO_7)$

Fig. 11. X-ray patterns of M3 pastes after 28-day hydration and after being exposed at different temperatures.

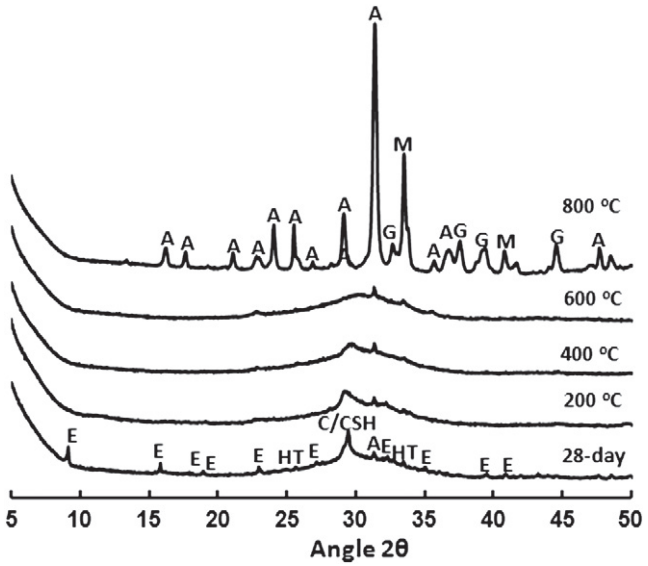

Key: E – ettringite $Ca_6Al_2(SO_4)_3(OH)_{12}\cdot 26H_2O$, HT – hydrotalcite $Mg_6Al_2CO_3(OH)_{16}\cdot 4H_2O$, C/C-S-H – overlapping calcite and calcium silicate hydrate, A – akermanite $Ca_2Mg(Si_2O_7)$, M –merwinite $Ca_3Mg(SiO_4)_2$, G-gehlenite $Ca_2Al(AlSiO_7)$

Fig. 12. X-ray patterns of M4 pastes after 28-day hydration and after being exposed at different temperatures.

C_2S and C_3S could be identified from XRD diagram which could be attributed to the decomposition of C-S-H [55,56].

Derivative thermogravimetric (DTG) thermograms of the hardened PC pastes at an ambient temperature and after being preheated at 200, 400, 600 and 800 °C are shown in Fig. 5. As can be seen from the DTG diagram, when the reference sample (28-day samples at an ambient temperature) was heated up to 1000 °C, three main endothermic regions can be identified. The first peak located at approximately 110–120 °C, is mostly due to the decomposition of C-S-H and ettringite. The second peak at approximately 500 °C is due to the decomposition of $Ca(OH)_2$; whilst the third peak at approximately 740 °C is due to the decarboxylation of calcite.

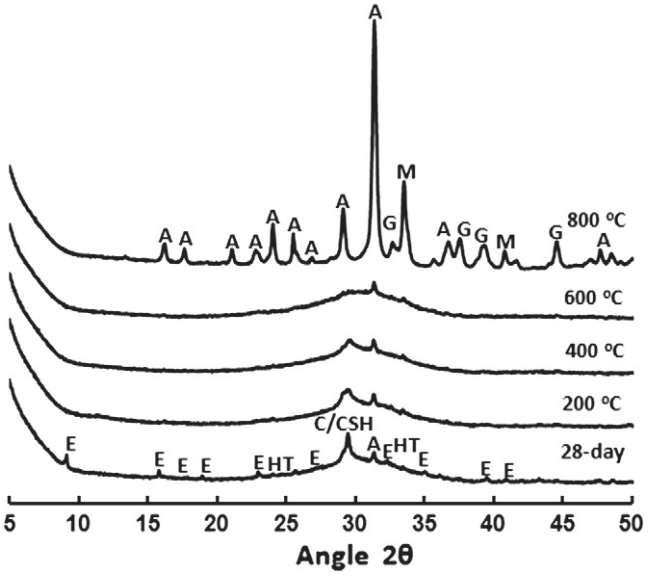

Key: E – ettringite $Ca_6Al_2(SO_4)_3(OH)_{12}\cdot 26H_2O$, HT – hydrotalcite $Mg_6Al_2CO_3(OH)_{16}\cdot 4H_2O$, C/C-S-H – overlapping calcite and calcium silicate hydrate, A – akermanite $Ca_2Mg(Si_2O_7)$, M –merwinite $Ca_3Mg(SiO_4)_2$, G-gehlenite $Ca_2Al(AlSiO_7)$

Fig. 13. X-ray patterns of M5 pastes after 28-day hydration and after being exposed at different temperatures.

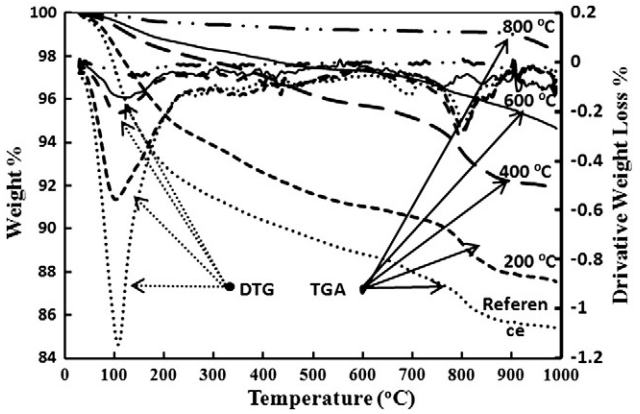

Fig. 14. Thermo-gravimetric analysis (TGA) and derivative thermogravimetric (DTG) curves for M5 after being exposed at different temperatures.

Similar patterns could be observed from those samples after being exposed to 200, 400, 600 and 800 °C. There is an increase in the endothermic peak around 500 °C for both the 200 and 400 °C samples, which could be attributed to the further hydration of the cement residues, leading to the increased amount of CH. This pattern correlates well with the XRD diagram. However, the peaks at 110–120 °C decreased for the samples subjected to 200 and 400 °C as the free and bound water from C-S-H gel is mainly evaporated during the temperature range of 100–300 °C. Most of the dehydration of ettringite should also have completed. Compared to the samples of the reference, 200 °C and 400 °C, the DTG peaks at around 500 °C decreased for the samples subjected to 600 and 800 °C. This is mainly due to the decomposition of calcium hydroxide around 500 °C.

3.3.2. Hardened sodium sulfate activated slag paste

Fig. 6 illustrates the residual and relative compressive strength results of activated slags made with both fine and coarse slags activated with 1% Na_2O equivalent of Na_2SO_4 for 28 days and after being exposed up to 800 °C. Overall, unlike the hardened PC pastes which increased in the strength up to 200 °C and then decreased up to 800 °C, the compressive strength of the activated slag mixes increased up to approximately 600 °C and after which point the strength decreased up to 800 °C. As a result, the activated slag pastes had higher relative strengths than PC pastes after being exposed to 200, 400 and 600 °C. The hardened paste made with the fine slag gave higher residual strength at all temperatures compared to the hardened paste made with the coarse slag.

Fig. 7 presents the evolution of residual compressive strength of the hardened slag pastes activated with 3% Na_2O equivalent of Na_2SO_4 which gave slightly higher residual strengths than those with 1% Na_2O equivalent of Na_2SO_4. It can be seen that these compressive strengths increased up to 600 °C, after that the strength decreased up to 800 °C. Use of higher dosage of the activator caused a slightly higher residual strength of the pastes made with fine slag than those made with coarse slag.

The above results are similar to those reported by Wang [12] where the compressive strength of a slag paste, made with a water/binder ratio of 0.47, increased as the exposure temperature increased up to 580 °C. In other works, Aydm [19] used pumice aggregate in mortars with PC/slag blended cement. The PC was replaced with slag at 20, 40, 60 and 80% whilst the water/binder ratios ranged from 0.7 to 0.72. The results indicated that, after exposure to the temperatures of 300 °C and 600 °C, the residual compressive strength was higher than the original strength but lower than that at 900 °C. These results reconfirmed those reported by Hooton and Emery [57] that heating up to 580 °C accelerated the hydration process for specimens containing slag.

Figs. 8 and 9 present the residual strength evolution as a function of the activator concentration and the slag fineness. These figures show that there was a slight increase in residual compressive strength with the higher concentration of Na_2SO_4 at 200, 600 and 800 °C. It is obvious that the compressive strength of M5 after being exposed to 600 °C and 800 °C is about 117.79% and 132.03% of the compressive strength of M3 after being exposed to the same temperatures, respectively. Evidently, as shown in Fig. 9, the same trend was observed for the pastes made with the coarse slag.

The XRD analysis of the pastes prior to exposure to elevated temperatures showed the presence of large amounts of C-S-H (I),

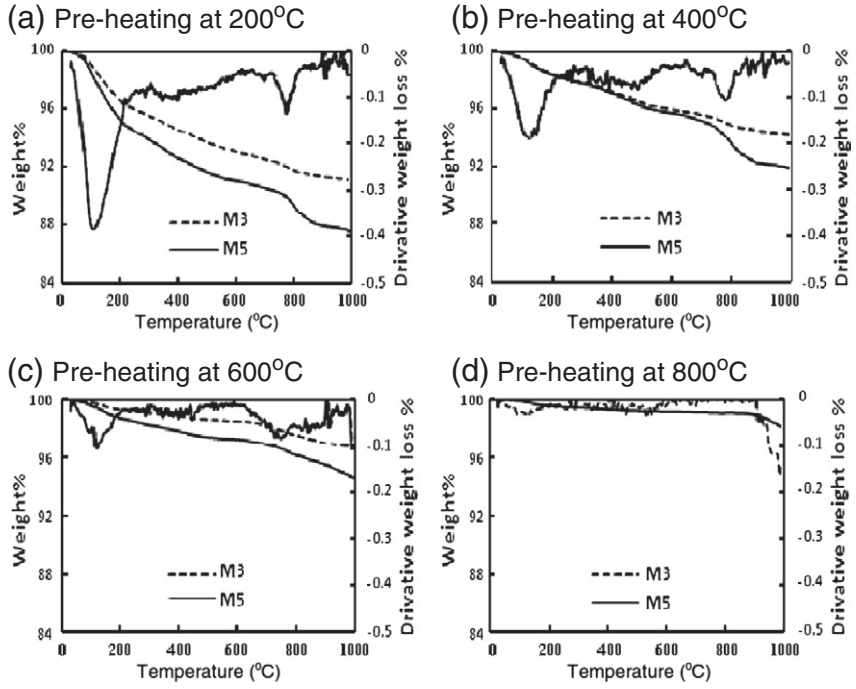

Fig. 15. Thermo-gravimetric analysis (TGA) and derivative thermogravimetric (DTG) curves for M3 versus M5 after being exposed to elevated temperatures.

together with traces of calcite ($CaCO_3$), ettringite ($Ca_6Al_2(SO_4)_3(OH)_{12}\cdot 26(H_2O)$), akermanite ($Ca_2Mg(Si_2O_7)$) and hydrotalcite ($Mg_6Al_2CO_3(OH)_{16}\cdot 4H_2O$) as shown in Figs. 10–13. Also presented in these figures are the XRD patterns for the samples after being treated at different temperatures. Overall, after the samples being heated at 200, 400 and 600 °C, the peaks for C-S-H/calcite reduced and became diffused compared to those of the reference samples. The peaks due to akermanite do not diminish unlike the peaks for ettringite and hydrotalcite. Instead, the intensity of the akermanite peaks increased in the samples heated to 800 °C along with the appearance of merwinite ($Ca_3Mg(SiO_4)_2$) and gehlenite $Ca_2Al(AlSiO_7)$. Similar results have been reported by Jiang et al. [58] when a slag was heated at 1450 °C. The conversion of C-S-H formed in waterglass activated slag into akermanite at elevated temperature was also reported by Zuda et al. [22].

The thermogravimetric analysis curves for the M5 pastes hydrated for 28 days and after being heated at 200, 400, 600 and 800 °C are shown in Fig. 14 with the corresponding DTG traces. For the reference sample, the main DTG peak centered at approximately 100 °C is due to the dehydration of C-S-H [59] but superimposed onto this peak could also be a small loss of water from ettringite [60]. The mass losses in the same temperature range for the samples exposed at 200, 400 and 600 °C were due to decomposition of C-S-H. For the sample heated at 800 °C there is a small peak in the range of 100–200 °C that represents the decomposition of C-S-H [61]. Peaks observed at approximately 800 °C in the reference sample and those exposed at 200, 400, and 600 °C were due to the decomposition of calcite but this phase was not present for the sample heated at 800 °C, presumably due to decomposition of calcite before 800 °C. The main feature of

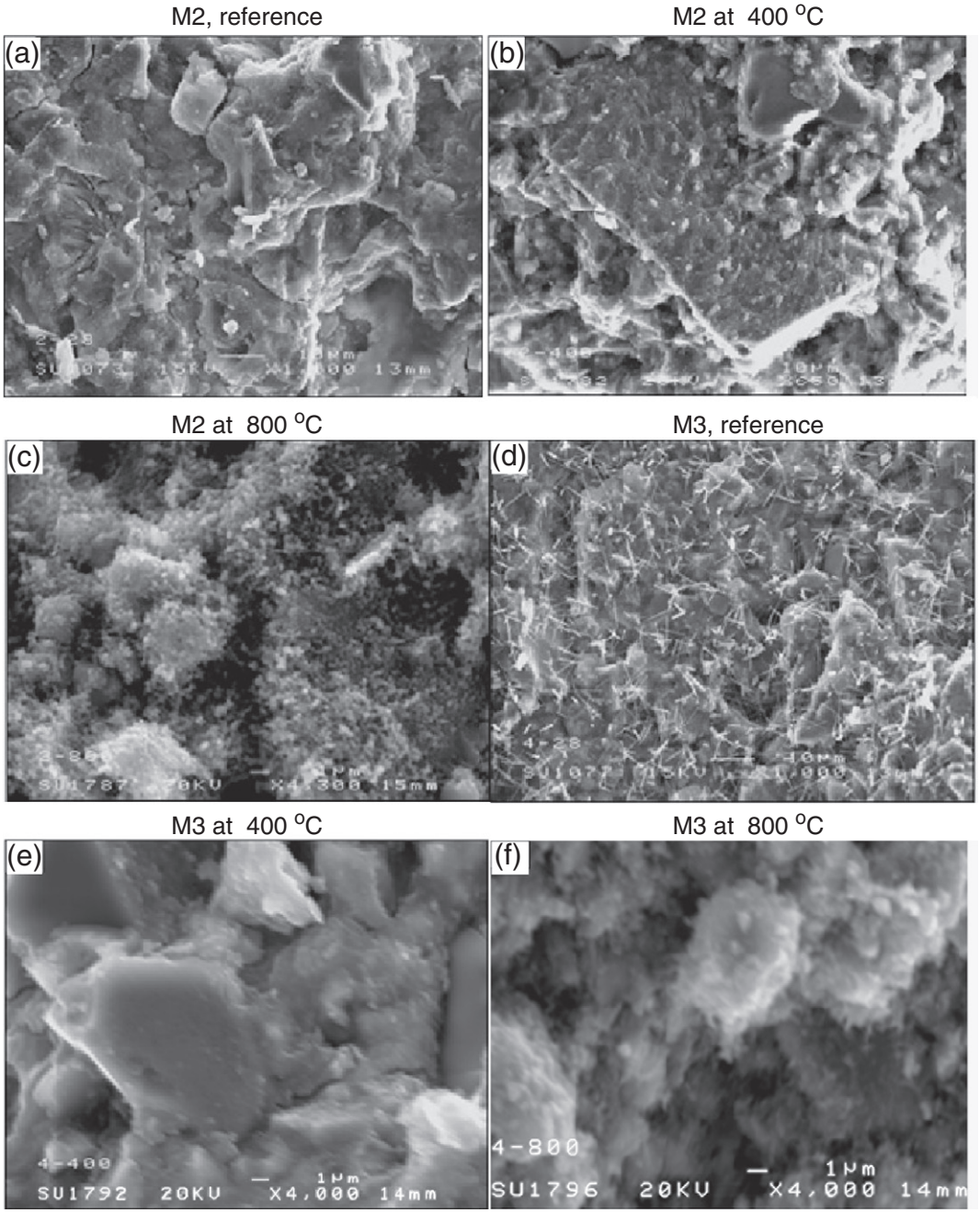

Fig. 16. SEM micrographs of hardened slag pastes activated with 1% Na_2O equivalent of Na_2SO_4 after being exposed at different temperatures.

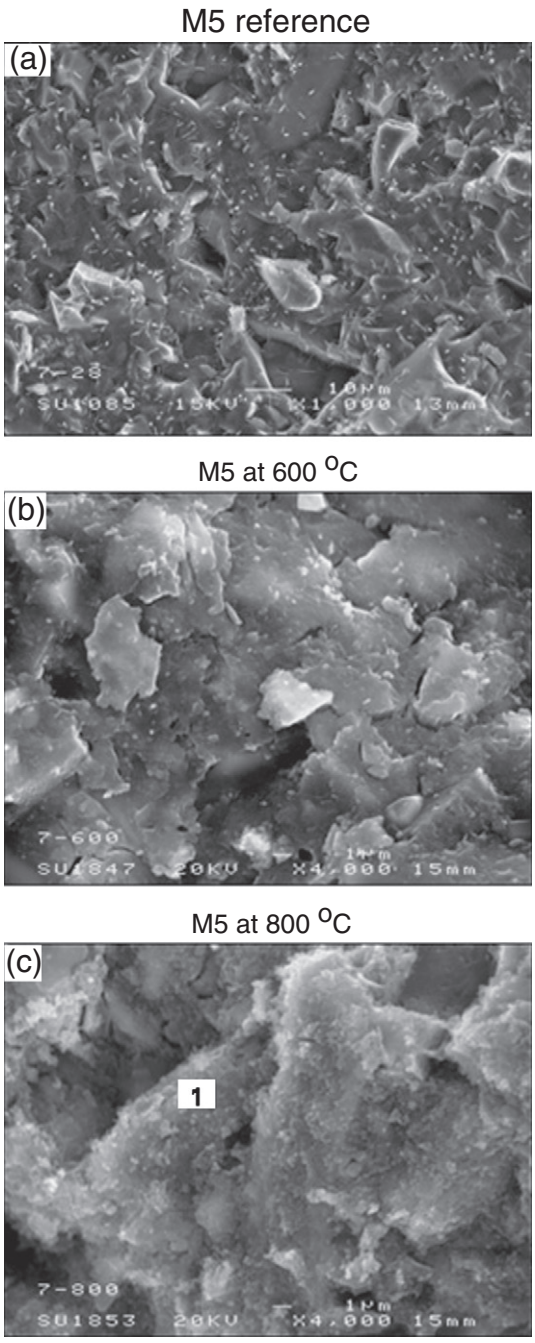

Fig. 17. SEM micrographs of hardened slag pastes activated with 3% Na_2O equivalent of Na_2SO_4 after being exposed at different temperatures.

Figs. 10–14 is that the Na_2SO_4 activated slags do not contain portlandite, which is the main element contributed to the strength deterioration at elevated temperatures for PC system. The previous results clearly showed that the absence of portlandite from the sodium sulfate activated slags led to better performance than the hardened PC pastes after exposure to elevated temperatures. This result seems to be similar to those from the alkali-activated slag systems where portlandite was also absent from the hydration products [20–23,28].

Fig. 15 shows the TGA and DTG curves for M3 versus M5. The DTG peaks for C-S-H are larger for M5 indicating that more hydration products were formed in the pastes activated with 3% Na_2O of Na_2SO_4.

Investigations of the microstructure of the hardened pastes using SEM showed distinct changes in morphology as a consequence of exposure to elevated temperatures. The microstructure of the coarse slag with 1% Na_2O equivalent of Na_2SO_4 cured at room temperature is shown in Fig. 16(a). This sample appeared to have a more porous microstructure and less C-S-H and ettringite formed than the fine slag activated with the same concentration of Na_2SO_4 as indicated in Fig. 16(d). After exposure to 400 °C, the microstructure of the paste manufactured with the coarse slag became more porous (as shown in Fig. 16(b)). Further increases in temperature up to 800 °C led to the formation of a weak structure of what may have been porous akermanite crystals (as shown in Fig. 16(c)).

In contrast, Fig. 16(d) shows a specimen prepared with the finer slag activated with 1% Na_2O equivalent where the microstructure is denser and contained many ettringite needles. Fig. 16(e) shows that the microstructure of this same sample after exposure to 400 °C, was denser than the coarse slag sample exposed to the same temperature. A further increase in temperature up to 800 °C resulted in a microstructure similar to that in Fig. 16(c) but with less apparent pores and lower porosity as shown in Fig. 16(f). These observations of porosity and microstructure correlated well with the residual compressive strength results.

Increasing the activator concentration from 1% to 3% [Na_2O equivalent of Na_2SO_4] in the fine slag appeared to produce more hydration products, with more ettringite needles and a denser microstructure as shown in Fig. 17(a). An SEM micrograph of the same hardened activated slag after exposure to 600 °C shows what appears to be C-S-H and angular slag particles (as shown in Fig. 17(b)). Fig. 17(c) shows the same sample after exposure to 800 °C which was similar to those shown in Fig. 16(c) and (f) but with less apparent pores and lower porosity. Fig. 18 shows the EDS trace of the spot marked 1 in Fig. 17(c) where the main elements detected were Ca and Si with smaller amounts of Mg and Al and a lesser extent of Si. The presence of Si and Ca as major peaks, and a lesser amount of Mg suggests the presence of akermanite ($Ca_2Mg(Si_2O_7)$).

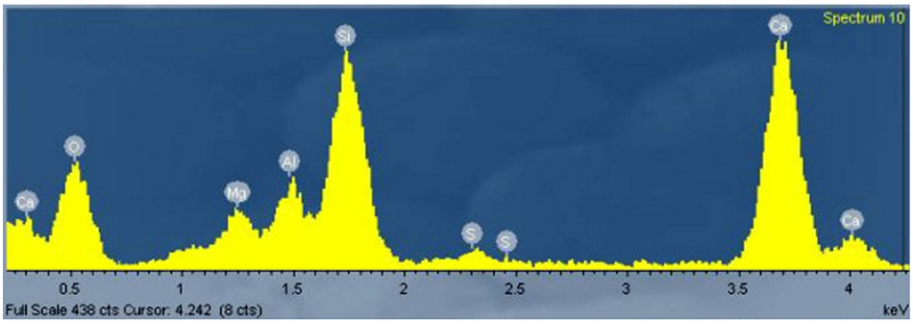

Fig. 18. EDS trace of the spot marked in Fig. 17(c).

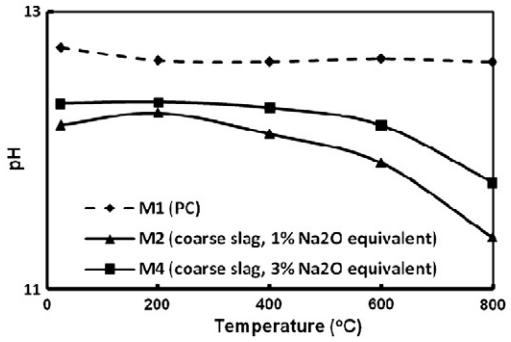

Fig. 19. Effect of elevated temperature on pH values for pastes made with PC and coarse slag activated with 1 and 3% Na_2O equivalent of Na_2SO_4.

3.3.3. pH values

In construction application, it is important to maintain a high pH in order to form a passive protective layer on the surface of reinforcing steel and, thereby, to reduce the risk of corrosion. The slag used in the current study had a pH value of approximately 11.5 when mixed with water, whilst the pH value of the Na_2SO_4 solution is 8.3 and 8.2 for 1 and 3% Na_2O equivalent respectively. However, the pH value of the pastes resulting from the activation of slag with Na_2SO_4 solutions appeared to be dependent on the concentration of the activator.

Figs. 19 and 20 show the pH of the reference samples and the samples after thermal treatment. A decrease in pH occurred with an increase in exposure temperature regardless of slag finenesses. Furthermore, increasing the concentration of activator led to an increase in pH, not only in the reference samples, but also after thermal treatment. These results seemed to be similar to the previous results that reported on alkali-activated fly ash by Rashad and Zeedan [43]. Figs. 19 and 20 also show that the reference PC sample had the highest value of pH (approximately 12.8) which decreased slightly to 12.2 after treatment at 800 °C. The pH of the activated slag samples started lower than those of PC and decreased faster after exposure to elevated temperatures reaching a value of approximately 11.4 at 800 °C. Although the pH values of the slag pastes were lower than those of PC pastes and decreased still further with an increase in temperature, the alkalinity was still high enough to maintain a passive layer on the surface of steel reinforcement even up to 800 °C. The lowest pH monitored was 11.34 after exposure to 800 °C (for M2) which still enables the passive layer forming on steel bars [62].

4. Conclusions

The results reported in this study provided new data on the fire performance of sodium sulfate activated slags after being exposed to temperatures up to 800 °C. The experimental and analytical studies have led to the following conclusions:

1. Sodium sulfate, is an effective activator for slag and paste workability was largely unaffected by activator concentration.
2. The sodium sulfate activated slag exhibited better chemical stability after being exposed to elevated temperature than PC system.
3. Compared to PC the sodium sulfate activated slag exhibited higher relative residual strength up to 600 °C so it appears more useful than PC as a fire resistant binder.
4. Both slag fineness and activator concentration have a marked influence on both the initial strength and the residual strength after heating.
5. After exposure to 800 °C, whilst the decomposition of C-S-H in PC system led to the formation of ß-C_2S and C_3S, akermanite, merwinite and gehlenite in the sodium sulfate activated slags.
6. The internal pH was affected by elevated temperatures. In PC this caused a slight decrease in pH but for the slag pastes there was a drop after 600 °C. However, this pH is sufficiently high to maintain a passive protective layer on the surface of reinforcing steel and to reduce the risk of corrosion.

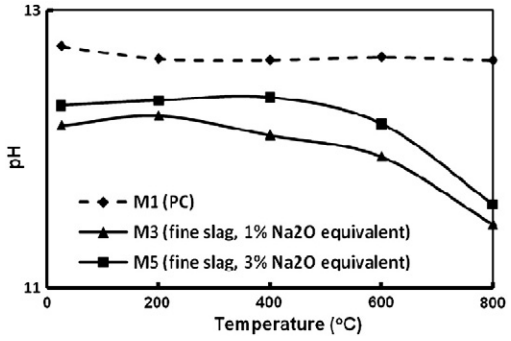

Fig. 20. Effect of elevated temperature on pH values for pastes made with PC and fine slag activated with 1 and 3% Na_2O equivalent of Na_2SO_4.

Acknowledgment

Dr A. M. Rashad was sponsored by the Egyptian government for his academic visit to Queen's University Belfast, U.K. The slag used in this research was supplied by Hanson Cement. This, and the facilities provided by the School of Planning, Architecture and Civil Engineering at Queen's University Belfast are also gratefully acknowledged.

References

[1] Hosam El-Din Seleem, Alaa M. Rashad, Tarek Elsokary, Effect of elevated temperature on physic-mechanical properties of blended cement concrete, Constr. Build. Mater. 25 (2011) 1009–1017.
[2] Hassan Hosny, Elmagd Abu, Fire in Concrete Building, Egyptian Universities Publishers, 1994.
[3] Z.P. Bazant, M.F. Kaplan, Concrete at High Temperatures—Material Properties and Mathematical Models, Longman, Group Limited, Essex, England, 1996 412.
[4] S.K. Handoo, S. Agarwal, S.K. Agarwal, Physicochemical, mineralogical, and morphological characteristics of concrete exposed to elevated temperatures, Cem. Concr. Res. 32 (2002) 1009–1018.
[5] B. Georgali, P.E. Tsakiridis, Microstructure of fire damaged concrete a case study, Cement Concr. Compos. 27 (2) (2005) 255–259.
[6] A. Petzold, M. Rohrs, Concrete for High Temperatures, 2nd ed. Maclaren and Sons Ltd, London, 1970.
[7] K.D. Hertz, Limits of spalling of fire-exposed concrete, Fire Saf. J. 38 (2) (2003) 103–116.
[8] V.K.R. Kodur, L.T. Phan, Critical factors governing the fire performance of high strength concrete systems, Fire Saf. J. 42 (6–7) (2007) 482–488.
[9] Y.N. Chan, G.F. Peng, M. Anson, Fire behavior of high-performance concrete made with silica fume at various moisture contents, ACI Mater. J. 96 (1999) 405–409.
[10] Andiç-Çakır Özge, Çopuroğlu Oğuzhan, Ramyar Kambiz, Effect of high temperature on mechanical and microstructural properties of cement mortar, 11DBMC International Conference on Durability of Building Materials and Components, Istanbul, Turkey 11–14, T11, May 2008.
[11] Civil and Marine is the UK'S major producer of GGBS, web site, http://www.civilandmarine.co.uk/1/home.htmlNov. 2008.
[12] H.Y. Wang, The effect of elevated temperature on cement paste containing GGBFS, Cem. Concr. Compos. 30 (2008) 992–999.
[13] A. Mendes, J.G. Sanjayan, F.G. Collins, Phase transformations and mechanical strength of OPC/Slag pastes submitted to high temperatures, Mater. Struct. 41 (2) (2008) 345–350.
[14] G.A. Khoury, B.N. Grainger, P.J.E. Sullivan, Transient thermal strain of concrete: literature review, conditions within specimen and behaviour of individual constituents, Mag. Concr. Res. 37 (132) (1985) 131–144.
[15] C.S. Poon, S. Azhar, M. Anson, Y.L. Wong, Comparison of the strength and durability performance of normal- and high-strength pozzolanic concretes at elevated temperatures, Cem. Concr. Res. 31 (9) (2001) 1291–1300.
[16] U. Diederichs, U.M. Jumppanen, V. Penttala, Behavior of high strength concrete at high temperatures, Report No. 92, Department of Structural Engineering, Helsinki University of Technology, 1989.
[17] P.J.E. Sullivan, R. Sharshar, Performance of concrete at elevated temperatures, Fire Technol. 28 (3) (1992) 240–250.
[18] J. Xiaoa, M. Xiea, C. Zhang, Residual compressive behaviour of preheated high-performance concrete with blast-furnace-slag, Fire Saf. J. 41 (2006) 91–98.

[19] S. Aydın, Development of a high-temperature-resistant mortar by using slag and pumice, Fire Saf. J. 43 (2008) 610–617.
[20] C.J. Shi, P.V. Krivenko, D.M. Roy, Alkali-activated Cements and Concretes, Taylor & Francis, 2006 376.
[21] U.M. Jumppanen, U. Diederichs, K. Hinrichsmeyer, Material properties of F-concrete at high temperatures, Research Report 452, Technical Research Centre of Finland, 1986.
[22] L. Zuda, Z. Pavlik, P. Rovnaníková, P. Bayer, R. Černý, Properties of alkali activated aluminosilicate material after thermal load, Int. J. Thermophys. 27 (2006) 1250–1263.
[23] Guerrieri Maurice, Sanjayan Jay, Collins Frank, Residual strength properties of sodium silicate alkali activated slag exposed to elevated temperatures, Mater. Struct. 43 (2010) 765–773.
[24] R.M. De Gutierrez, J. Maldonado, C. Gutierrez, Performance of alkaline activated slag at high temperatures, Materiales De Construccion 54 (276) (2004) 87–92.
[25] P. Rovnanikova, P. Bayer, P. Rovnanik, J. Novak, Properties of alkali activated aluminosilicate materials with fireresistant aggregate after high temperature loading, Cement Combinations for Durable Concrete: Proceedings of the International Conference, Dundee, U.K., 2005, 277–286.
[26] P. Rovnanik, P. Bayer, P. Rovnanikova, New possibilities of fire protection of tunnel walls, Concrete Structures for Traffic Network: Proceedings of the 2nd Central European Congress on Concrete Engineering, Hradec Kralove, Czech Republic, 2006, 496–501.
[27] L. Zuda, P. Rovnanikova, P. Bayer, R. Cerny, Thermal properties of alkali activated slag subjected to high temperatures, J. Build. Phys. 30 (4) (2007) 337–350.
[28] Guerrieri Maurice, Sanjayan Jay, Collins Frank, Residual compressive behavior of alkali-activated concrete exposed to elevated temperatures, Fire and Materials (2008), doi:10.1002/fam.983.
[29] A. Bernal Susan, D. Rodríguez Erich, Mejía de GutieérrezRuby, Marisol Gordillo, John l Provis, Mechanical and thermal characterization of geopolymers based on silicate-activated metakaolin/slag blends, J. Mater. Sci. (2011), doi:10.1007/s10853-011-5490-z.
[30] T.W. Cheng, J.P. Chiu, Fire-resistance geopolymer produced by granulated blast furnace slag, Miner. Eng. 16 (2003) 205.
[31] Palacios M., (2008) Consejo superior de investigacions científicas, Ph.D thesis, Universidad Autónoma de Madrid, Spain.
[32] Zuda Lucie and Čemý Robert, Measurement of linear thermal expansion coefficient of alkali-activated aluminosilicate composites up to 1000 °C, Cem. Concr. Compos. 31 (4) (2009) 263–267.
[33] M.S. Morsy, A.F. Galal, S.A. Abo-El-Enein, Effect of temperature on phase composition and microstructure of artificial pozzolana-cement pastes containing burnt kaolinite clay, Cem. Concr. Res. 28 (8) (1998) 1157–1163.
[34] M.M. Shoaib, S.A. Ahmed, M.M. Balaha, Effect of fire and cooling mode on the properties of slag mortars, Cem. Concr. Res. 31 (2001) 1533–1538.
[35] A. Savva, P. Manita, K.K. Sideris, Influence of elevated temperatures on the mechanical properties of blended cement concretes prepared with limestone and siliceous aggregates, Cem. Concr. Compos. 27 (2005) 239–248.
[36] Zuda Lucie, Rovnaník Pavel, Bayer Patrik, Černý Robert, Effect of high temperatures on the properties of alkali activated aluminosilicate with electrical porcelain filler, Int. J. Thermophys. 29 (2008) 693–705.
[37] M.S. Morsy, A.M. Rashad, S.S. Shebl, Effect of elevated temperature on compressive strength of blended cement mortar, Build. Res. J. 56 (2–3) (2008) 173–185.
[38] M.S. Morsy, A.M. Rashad, H.A. El-Nouhy, Effect of elevated temperature on physic-mechanical properties of metakaolin blended cement mortar, Struct. Eng. Mech. 31 (1) (2009) 1–10.
[39] M.S. Morsy, S.S. Shebl, A.M. Rashad, Effect of fire on microstructure and mechanical properties of blended cement pastes containing metakaolin and silica fume, Sil. Ind. 74 (3–4) (2009) 59–64.
[40] M. Fall, S.S. Samb, Effect of high temperature on strength and microstructural properties of cemented paste backfill, Fire Saf. J. 44 (2009) 642–651.
[41] Zuda Lucie, Drchalová Jaroslava, Rovnaník Pavel, Bayer Patrik, Keršner Zbyněk, Černý Robert, Alkali-activated aluminosilicate composite with heat-resistant lightweight aggregates exposed to high temperatures: mechanical and water transport properties, Cem. Concr. Compos. 31 (2010) 157–163.
[42] Mandal Kalyan Kr, Thokxhom Suresh, Roy Mithun, Effects of Na_2O content on performance of fly ash geopolymers at elevated temperature, Int. J. Civ. Environ. Eng. 3 (1) (2011) 34–40.
[43] Alaa M. Rashad, Sayieda R. Zeedan, The effect of activator concentration on the residual strength of alkali-activated fly ash pastes subjected to thermal load, Constr. Build. Mater. 25 (2011) 3098–3107.
[44] F. Collins, J.G. Sanjayan, Early age strength and workability of slag pastes activated by NaOH and $N_{a2}C_{O3}$, Cem. Concr. Res. 28 (5) (1998) 655–664.
[45] L.T. Phan, Fire performance of high strength concrete, A Report of the State-of-the-art, Building and Fire Research Laboratory, National Institute of Standards and Technology, Maryland, 1996.
[46] G.A. Khoury, Compressive strength of concrete at high temperatures: a reassessment, Mag. Concr. Res. 44 (161) (1992) 291–309.
[47] W.P.S. Dias, G.A. Khoury, P.J.E. Sullivan, Mechanical properties of hardened cement paste exposed to temperatures up to 700 °C, ACI Mater. J. 87 (2) (1990) 160–166.
[48] K.M.A. Hossain, High strength blended cement concrete incorporating volcanic ash: performance at high temperatures, Cem. Concr. Compos. 28 (2006) 535–545.
[49] P. Nimityongskul, T.U. Daladar, Use of coconut husk ash, corn cob ash and peanut shell ash as cement replacement, Journal of Ferrocement 25 (1) (January 1995) 35–44.
[50] I.C. Neves, F.A. Branco, J.C. Valente, Effects of formwork fires in bridge construction, Concr. Int. 19 (1997) 41–46.
[51] P.S. Rostasy, R. Weiss, G. Wiedemann, Changes of pore structure of cement mortars due to temperatures, Cem. Concr. Res. 10 (1980) 157–164.
[52] H. Wood, Durability of concrete construction, ACI & The Iowa State University Press, USA, 1968.
[53] Peng Gai-Fei, Peng Zhi-Shan, Change in microstructure of hardened cement paste subjected to elevated temperatures, Constr. Build. Mater. 22 (2008) 593–599.
[54] M. Collepardi, The New Concrete published by, Grafiche Tinoretto–Vicolo Verdi 45/47, Castrette di Villorba TV, Italy, 2006 First Published.
[55] H.F.W. Taylor, Cement Chemistry, Academic Press, New York, 1990.
[56] G.F. Peng, S.Y.N. Chan, M. Anson, Decomposition in hardened cement paste subjected to elevated temperatures up to 800 °C, Adv. Cem. Res. 13 (No. 2) (April 2001) 47052.
[57] R.D. Hooton, J.J. Emery, Glass content determination and strength development predictions for vitrified blast furnace slag, fly ash, silica fume and other mineral by-products in concrete, American Concrete Institute, 1983 943–62.
[58] W. Jiang, M.R. Silsbee, D.M. Roy, Similarities and differences of microstructure and macro properties between Portland and blended cement, Cem. Concr. Res. 27 (10) (1997) 1501–1511.
[59] H.F.W. Taylor, Cement Chemistry, Thomas Telford Ltd., London, 1997.
[60] K.T. Greene, Early hydration reactions of Portland cement, Proceedings of the fourth International Symposium on Chem. Cements, Washington, 1960 p. 359.
[61] K.L. Lin, K.S. Wang, T.Y. Lee, B.Y. Tzeng, The hydration characteristics of MSWI fly ash slag present in C_3S, Cem. Concr. Res. 33 (2003) 957–964.
[62] Böhni Hans, (2005) "Corrosion in reinforced concrete structures", CRC Press, Boca Raton Boston New York Washington, Woogead Publishing Limited, Cambridge England.